Article

Not peer-reviewed version

Assessing Recession Constant Sensitivity and Its Interaction with Data Adjustment Parameters in Continuous Hydrological Modeling in Data Scarce Basins: A Case Study Using the Xinanjiang Model

Thandar Tun Zin * , Minjiao LU , Takahiro OGURA

Posted Date: 1 December 2023

doi: 10.20944/preprints202312.0058.v1

Keywords: XAJ model; Recession constant; Data adjustment parameter; Model performance; Sensitivity

 doi:10.20944/preprints202312.0058.v1

Article

Assessing Recession Constant Sensitivity and Its Interaction with Data Adjustment Parameters in Continuous Hydrological Modeling in Data Scarce Basins: A Case Study Using the Xinanjiang Model

Thandar Tun Zin *, Minjiao Lu and Takahiro Ogura

Department of Civil and Environmental Engineering , Nagaoka University of Technology, 1603-1, Kamitomioka,Nagaoka, 940-2188, Niigata, Japan

* Correspondence: s207009@stn.nagaokaut.ac.jp

Abstract: While considering the sensitivity over the parameter optimization, it is essential to determine which parameters have the most significant implications on model performance. This study focuses on the baseflow recession constant as one of the independent basin parameters to forecast low flows, perform hydrograph analysis, and calibrate rainfall-runoff models for significant improvement. Prior studies examined that the optimization of data adjustment parameters can improve the hydrological model performance and determine the minimum acceptable data length for data scarce regions using the Xinanjaing model. However, it is essential to pay special attention to the sensitivity of the recession constant, which can also impact the model performance during the data scarcity. Therefore, this study extends the research to comprehend the recession constant sensitivity over data adjustment parameters in the shorter datasets leading to more reliable parameter estimation. In terms of that, this study explores how recession constant affects hydrological parameter estimation on annual scale while keeping data adjustment parameters constant in continuous hydrological modeling, employing the Xinanjiang (XAJ) model as a case study. This study considered two approaches of recession constant (c_g); (i) assessing the relationship between c_g and the data adjustment parameter (C_{ep}), for the 28-year datasets, (ii) investigating the significant impacts of the sensitivity of c_g over C_{ep} in shorter datasets which can affect the estimation of the acceptable minimum data length in the data scarce basins. The study underscores the importance of the recession constant sensitivity for reliable continuous hydrological model predictions, especially in data-scared areas. The study's outcomes enhance the understanding of the importance of parameter sensitivity and its relationship in conceptual hydrological modeling during the data limitations.

Keywords: XAJ model; recession constant; data adjustment parameter; model performance; sensitivity

---

1. Introduction

Hydrological models have been regarded as a powerful and essential tool for handling water and environmental resources as the magnitude of harm they inflict are increasing in both financial and social aspects[1]. In this context, hydrological modeling methods are advanced tremendously in terms of complexities with a wide range of application areas, including the study of the climate change and land use paradigm, flood forecasting, and rainfall-runoff modeling [2–5]. Assessing the modeling process's uncertainty and quantifying it contributes in assessing how reliable the predictions remain. To make reliable decisions, model users and decision-makers need to be aware of the possible range of outcomes. Uncertainties within hydrological modeling play the vital role in many regions, especially in developing countries, where the data scarcity and data limitations can impact the model calibration predictions. Consequently, the importance of understanding the uncertainties within hydrological modeling has grown significantly [6–8].

In the domain of hydrological study, modeling uncertainties can be categorized into three major

 doi:10.20944/preprints202312.0058.v1

groups, known as: (i) data uncertainty, (ii) model structure uncertainty, and (iii) parameter uncertainty [9–12]. Among these, parameter uncertainties arising from the challenges of optimizing model parameters and model estimation are frequently identified in recent studies. Since the majority of model parameters are difficult to predict precisely, they need to be evaluated through a calibration procedure using the available data. Addressing the issues associated with parameter uncertainties in hydrological modeling has been a major focus in recent studies [13–15]. However, identifying suitable parameter values to manage uncertainty in parameter estimation becomes challenging due to limited data availability in hydrological modeling, especially in many developing and underdeveloped countries [6–8,16]. Parameter estimation during data scarcity can lead to inadequate model performance, overparameterization, and poor model robustness. In addition, recent literature on hydrological model calibration demonstrates that improvements are needed in the existing calibration approaches' process representation, spatial prediction, and runtime efficiency in the case of data scarcity [17].To address the above identified issues, it is crucial to detect the sensitive parameters in model calibration and parameter optimization in the data scarce basins.

Conceptual hydrological models are one example of how actual process models continuously improve to effectively represent the underlying uncertainties associated with inputs, parameters, and the presumed model validation [18–25]. In addition, conceptual models specialize in minimal data requirements and broad applicability in real-world hydrology [26].In this context, this study utilized the XAJ, a widely used probability-distributed model for hydrological studies, to evaluate the most influential parameters [27,28].Given the data adjustment and linear reservoir recession are common parts in many widely used hydrological models, e.g., the NWS River Forecast System - Catchment Modeling and TANK Model [29], the results of this study are of general applicability and not limited to the XAJ model.According to recent studies, Lu and Li (2014) examined parameter sensitivities within the Xinanjiang (XAJ) model using global sensitivity analysis techniques across different timescales for model calibration improvement. Their work notably highlighted the increased sensitivity of the recession constant on an annual timescale while data adjustment parameters remained constant.

Through this research initiative, we aim to validate the relationship between the data adjustment parameter (C_{ep}) and the recession constant (c_g) while only limited datasets are available, highlighting the critical role of recession constant sensitivity. As inaccurate parameter estimation due to data scarcity can lead to poor model calibration and performance, current research initially aims to prove the interaction of the data adjustment parameter (C_{ep}) with the recession constant (c_g) in 28-year dataset to highlight the importance of the sensitivity of the recession constant in hydrological modeling. Next, it offers valuable insights into the significant impact of c_g on C_{ep} within shorter subsets, seeking to address the constraints posed by these influences on parameter estimation and the determination of the acceptable minimum data length, particularly in data-scarce regions. This approach can identify which parameters influence the model's calibration and performance without over-parameterization [30].

2. Materials and Methods

2.1. Study Basins

Five river basins in the USA (MOPEX ID: 903504000, MOPEX ID: 902387500, MOPEX ID: 902472000, MOPEX ID: 903443000, and MOPEX ID: 911532500) are investigated during this research including the same two basins from the recent study [31]. According to the study, these basins possess robust datasets, and the XAJ model could accurately estimate their runoff. Assessing to include the same two basin permits comparing the parameter optimization and the minimum data length estimation from two different approaches. Furthermore, it provided a way to correlate the relationship between parameter sensitivity with model performance. Table 1 illustrates a brief overview of the physical characteristics of the researched basins.

Preprints (www.preprints.org) | NOT PEER-REVIEWED | Posted: 1 December 2023 doi:10.20944/preprints202312.0058.v1

Table 1. Studied MOPEX basins, locations and basin characteristics.

	Location						
MOPEX ID	**Long**	**Lat**	**State**	**Drainage area (Sq.km)**	**Data length (year)**	**MP(mm/year)**	**MPE(mm/year)**
903504000	-83.62	35.13	NC	135.00	28	1893	762.00
902387500	-84.94	34.58	GA	4144.0	28	1480	901.00
902472000	-89.41	31.71	MS	1924.0	28	1492	1060.0
903443000	-83.62	35.29	NC	740.00	28	2156	817.00
911532500	-124.05	41.79	CA	1577.0	28	2687	740.00

* indicates the selected basins in Alabama, USA; including Mean Precipitation (MP) and Mean Potential Evapotranspiration (MPE).

2.2. Data Description

The U.S. MOPEX dataset [32] was used to develop the basin scale daily precipitation, P (daily mean aerial precipitation calculated from ground-based gauge precipitation), potential evaporation, E_p (developed from NOAA Evaporation Atlas), and discharge, Q (developed from USGS hydro-climatic data) information utilized in this research openly available at ftp://hydrology.nws.noaa.gov/ (accessed on 19 October 2013). Table 2 provides comprehensive descriptive data statistics of the examined basins.

Considering the lack of data and limitations in practical modelling research, the XAJ model is calibrated using 28-year datasets and subsets from each basin to highlight the model's effectiveness. For subsets, 28-year datasets are divided into shorter data lengths with different year intervals starting from 6-year to 28-year subsets[31].

Here, we defined the input datasets $I^{n,m}$ including P and E_p, and $Q^{n,m}_{obs}$ as the observed runoff, where n is the length of datasets and m is the number of subsets ($m = 1, 2, ..., 28 - n + 1$).

2.3. XAJ Model and Parameter Description

In this study, we used the Xinanjiang model, a conceptual hydrological model, designed by the Flood Forecast Research Institute of the East Chinese Technical University of Water Resources [33]. This model is utilized for humid and semiarid areas of China to estimate runoff generation within a basin [33,34]. The physical meaning of the model is robust. The simulated XAJ model utilized in this research comprises fifteen parameters as referred in Table 3 [33,35,36]. The complexity of the connections and interactions among the numerous parameters required in calibration can be minimized by the level of parameter estimation.

Here, the estimation of data adjustment parameter, C_{ep}, is detailed through the aridity index method[37] while the calculation of the recession constant parameter, c_g, employs the time constant, T. ϕ_0 denote the pre-optimized parameter vector as in Table 2 .

Let the function specify the XAJ model calibration, X and let the input datasets comprise the vector $I^{n,m}$ where n is the length of datasets and m is the number of subsets. Let the simulated runoff by the XAJ model calibration for $I^{n,m}$ be specified by the following equation:

$$Q^{n,m}_{cal} = X(I^{n,m}, C_{ep}, c_g \mid \phi_0) \tag{1}$$

where C_{ep} represents the adjustment parameter (the most sensitive parameter at the annual scale in the XAJ model), c_g is the recession constant (sensitive at the annual scale when the adjustment parameters are kept constant), ϕ_0 represents the application of 13 pre-optimized parameter values, a subset of all 15 parameters in the XAJ model. These parameters are fixed in this study. As these parameter values are not inferred through the calibration process, ϕ_0 will be excluded from the following equation for clarity.

$$Q^{n,m}_{cal} = X(I^{n,m}, C_{ep}, c_g) \tag{2}$$

Preprints (www.preprints.org) | NOT PEER-REVIEWED | Posted: 1 December 2023 doi:10.20944/preprints202312.0058.v1

Table 2. Descriptive statistics of studied basins

MOPEX ID	Mean precipitation (mm/year)	Median precipitation (mm/year)	Minimum precipitation (mm/year)	Maximum precipitation (mm/year)	Standard Deviation
903504000	1890	2051.98	1427.09	4424.72	571.450
902387500	1480	1481.05	1046.53	1930.67	228.240
902472000	1492	1550.62	1135.21	4615.13	674.880
903443000	2156	2064.90	1349.55	6646.70	1018.10
911532500	2687	2718.04	1644.96	7172.92	1176.72

2.4. Relationship Between Data Adjustment Parameter (C_{ep}) and the Recession Constant (c_g)

According to the general water balance equation for vertical water flux, the relationship between the adjustment parameter and the recession constant parameter can be observed as shown in the following equation,

$$C_p P_g = C_{ep} E_p + R + \Delta S \tag{3}$$

where P_g is the actual rainfall calculated from a ground-based rain gauge, E_{pan} is the annual evaporation, R is the annual runoff depth, and ΔS is the changes in water storage.

However, in this study, we considered that the baseflow storage can be affected by the recession constant c_g at the beginning and end of the year under certain circumstances. To resolve this approach, ΔS must be taken into consideration, which is a highly subjective task that might have significant effects on the close relationship between C_{ep} and c_g.

2.5. Assessment of Recession Constant, (c_g)

Three runoff components of surface runoff, interflow, and baseflow, are routed using three linear reservoirs as follows:

$$Q_x\,(t+1) = c_x Q_x\,(t) + \ (1-c_x)\,R_x \qquad x = s, i, g \tag{4}$$

where subscript x indicates runoff component, s for surface flow,i for interflow, and g for baseflow c_s, c_i and c_g are their recession coefficients.Usually,

$$0 < c_s < c_i < c_g < 1$$

According to [34], among 15 parameters, the most sensitive parameter at the annual scale while keeping C_p and C_{ep} constants is c_g. In this study, the values of c_g were calculated using the time constant not to exceed the limits between 0 and 1. T is related to c_g by the following expression,

$$T = \ {}^{-\Delta t}/_{\ln c_g} \tag{5}$$

whereas T is the time constant constant of the baseflow system in days, c_g is the recession constant in t dimensionless quantity whose value depends on the time unit chosen.

2.6. Assessment of Data Adjustment Parameter, (C_{ep})

Li and Lu [37] emphasize that this study predominantly uses the aridity index method. Correlating runoff coefficient and data aridity could support the reduction of parameter space for C_p and C_{ep} rather than separate assessments. To reduce such inaccuracy and improve the efficiency of parameter estimation, the interaction between the runoff coefficient and the data aridity index is applied to parameter estimation.

Within the limitations of the pan aridity index and annual runoff coefficient, the values of C_p and C_{ep}

Preprints (www.preprints.org) | NOT PEER-REVIEWED | Posted: 1 December 2023 doi:10.20944/preprints202312.0058.v1

might be determined.

In the logarithm form,

$$\ln\left({}^{R}/{}_{P_g}\right) = -\alpha\left({}^{C_{ep}}/{}_{C_p}\right)\zeta_{g,pan} + \ln C_p \tag{6}$$

Here, estimation for 28-year datasets and subsets is outlined by function Y, $C_{ep}^{n,m}$ represent the estimated C_{ep} values for subsets, $I^{n,m}$. The subsequent equation explains data adjustment parameter estimation in subsets, $I^{n,m}$.

$$C_{ep}^{n,m} = Y(Q_{obs}^{n,m}, I^{n,m}) \tag{7}$$

2.7. Evaluation of Model Performance Using Nash-Sutcliffe Efficiency

The Nash and Sutcliffe (1970) coefficient of efficiency is widely used in the evaluation of hydrological modelling [38–43]. Simulated runoff information is derived utilizing well-known Nash-Sutcliffe efficiency [44].

The definition of Nash-Sutcliffe efficiency is as follows;

$$NSE = 1 - \frac{\sum_{t=1}^{n}\left(Q_{obs}(t) - Q_{cal}(t)\right)^2}{\sum_{t=1}^{n}\left(Q_{obs}(t) - \overline{Q_{obs}}\right)^2} \tag{8}$$

where Q_{cal} is the simulated runoff, Q_{obs} is the observed runoff, and $\overline{Q_{obs}}$ is the mean value of observed runoff.

This study calculates the observed and simulated runoff from the XAJ model driven by 28-year datasets and subsets, $I^{n,m}$. It can be expressed as follows:

$$NSE^{n,m} = NSE(Q_{obs}^{n,m}, Q_{cal}^{n,m}) \tag{9}$$

where $Q_{obs}^{n,m}$ are the daily observed runoff.

At an annual scale, the parameters affecting the $Q_{cal}^{n,m}$ are mainly C_{ep} and c_g. Equation (9) can also be written in the following function:

$$NSE^{n,m} = NSE(C_{ep}^{n,m}, c_g^{n,m} \mid Q_{obs}^{n,m}, \phi_0) = NSE(C_{ep}^{n,m}, c_g^{n,m}) \tag{10}$$

2.8. Application of Data Adjustment Parameter and Recession Constant in Model Calibration

The simulated recession constant, $c_{g,ref}$, is initially estimated using the linear polynomial regression analysis. The values of $c_{g,ref}$ were selected based on the c_g values with the best model performance in the longest datasets.

$$NSE(C_{ep}^{28,1}, c_{g,ref}) \geq NSE(C_{ep}^{28,1}, c_g) \tag{11}$$

where $C_{ep}^{28,1}$ refers to the estimated adjustment parameter value using a 28-year data length.

Preprints (www.preprints.org) | NOT PEER-REVIEWED | Posted: 1 December 2023 doi:10.20944/preprints202312.0058.v1

Table 3. Description of the parameters in the Xinanjiang model.

Parameter	Physical meaning	Range	Pre-optimized values, ϕ_0				
			MOPEX ID				
			903504000	**902387500**	**902472000**	**903443000**	**911532500**
Group I							
C_p	Ratio of measured precipitation to actual precipitation	0.8–1.2	1	1	1	1	1
C_{ep}	Ratio of potential evaporation to pan evaporation	0.8–1.2	0.7908	1.25	1.2806	0.9865	0.7184
Group II							
SM	Areal mean free water capacity of the surface soil layer (mm)	1–50	40	30	50	40	30
EX	Areal mean of the free water capacity of the surface soil layer (mm)	0.5–2.5	1.2	0.5	0.5	1.2	0.5
KI	Outflow coefficients of the free water storage to interflow	0–0.7; KI + KG = 0.7	0.1	0.3	0.55	0.1	0.3
KG	Outflow coefficients of the free water storage to groundwater	0–0.7; KI + KG = 0.7	0.6	0.4	0.15	0.6	0.4
c_s	Recession constant of the lower interflow storage	0.5–0.9	0.6	0.85	0.75	0.6	0.4
c_i	Recession constant for the lower interflow storage	0.5–0.9	0.9	0.75	0.8	0.9	0.75
c_g	Recession constant of the groundwater storage	0.9835–0.998	0.98	0.987	0.983	0.98	0.983

Preprints (www.preprints.org) | NOT PEER-REVIEWED | Posted: 1 December 2023 doi:10.20944/preprints202312.0058.v1

Table 3. *Cont.*

Parameter	Physical meaning	Range	Pre-optimized values, ϕ_0				
			MOPEX ID				
Group III			**903504000**	**902387500**	**902472000**	**903443000**	**911532500**
b	Exponent of the tension water capacity curve	0.1–0.3	0.3	0.15	0.15	0.3	0.15
imp	Ratio of the impervious to the total area of the basin	0–0.005	0.02	0.01	0.01	0.02	0.01
WUM	Water capacity in the upper soil layer (mm)	5–20	20	20	20	20	20
WLM	Water capacity in the lower soil layer (mm)	60–90	80	80	80	80	80
WDM	Water capacity in the deeper soil layer (mm)	10–100	60	160	160	160	160
C	Coefficient of deep evapotranspiration	0.1–0.3	0.15	0.15	0.15	0.15	0.15

Note: ϕ_0 indicates the pre-optimized parameter values.

Preprints (www.preprints.org) | NOT PEER-REVIEWED | Posted: 1 December 2023 doi:10.20944/preprints202312.0058.v1

To highlight the sensitivity impact of the recession constant in shorter datasets, the data adjustment parameter values for subsets are essential to optimize the recession constant values for subsets. To compare the impacts of parameter sensitivity in shorter data length, we first identify the estimated C_{ep} values for subsets based on three conditions: maximum, minimum and median annual model results, NSE. Let $C^{n,m}_{ep,best}$, $C^{n,m}_{ep,worst}$ and $C^{n,m}_{ep,median}$ be the maximum, minimum and median $C^{n,m}_{ep}$ values in subsets ($I^{n,m}$), when running the model using $c_{g,ref}$.
The maximum, minimum and median annual NSE, can be specified using $C^{n,m}_{ep}$ and $c_{g,ref}$ in subsets using by the following equations,

$$max(NSE(C^{n,m}_{ep}, c_{g,ref})) = NSE(C^{n,m}_{ep,best}, c_{g,ref}) \tag{12}$$

$$min(NSE(C^{n,m}_{ep}, c_{g,ref})) = NSE(C^{n,m}_{ep,worst}, c_{g,ref}) \tag{13}$$

$$median(NSE(C^{n,m}_{ep}, c_{g,ref})) = NSE(C^{n,m}_{ep,median}, c_{g,ref}) \tag{14}$$

For the comparison of the sensitivity influence of recession constants over the parameter estimation in shorter data length, we apply the maximum, minimum and median calibrated data adjustment parameter values ($C^{n,m}_{ep,best}$, $C^{n,m}_{ep,worst}$ and $C^{n,m}_{ep,median}$) in model calibration to receive the maximum, minimum and median recession constant values ($c^{n,m}_{g,best}$, $c^{n,m}_{g,worst}$ and $c^{n,m}_{g,median}$) in subsets. Finally, the maximum, minimum and median annual NSE results using $c^{n,m}_{g,best}$, $c^{n,m}_{g,worst}$ and $c^{n,m}_{g,median}$ are estimated by comparing NSE results with $c_{g,ref}$ using the following equations.

$$NSE(C^{n,m}_{ep,best}, c^{n,m}_{g,best}) \geq NSE(C^{n,m}_{ep,best}, c_{g,ref}) \tag{15}$$

$$NSE(C^{n,m}_{ep,worst}, c^{n,m}_{g,worst}) \geq NSE(C^{n,m}_{ep,worst}, c_{g,ref}) \tag{16}$$

$$NSE(C^{n,m}_{ep,median}, c^{n,m}_{g,median}) \geq NSE(C^{n,m}_{ep,median}, c_{g,ref}) \tag{17}$$

where $c^{n,m}_{g,best}$, $c^{n,m}_{g,worst}$ and $c^{n,m}_{g,median}$ are calculated based on the maximum, minimum and median model outputs while running with $C^{n,m}_{ep,best}$, $C^{n,m}_{ep,worst}$ and $C^{n,m}_{ep,median}$ with $c_{g,ref}$.

2.9. Application of Linear Polynomial Regression Analysis for Data Comparison

In this study, polynomial regression analysis was applied to attain and analyse the relationship between c_g and annual Nash using both 28-year datasets and subsets to access the the best approximation between these two parameter values[45–47].

3. Results and Discussions

The effect of data scarcity on parameter estimation plays as one of the most important factors which influences the model's reliability and precision. Therefore, in designing long-term hydrological models, the time-related character of sensitivity should be considered [48]. In this research, the performance of the data adjustment parameter estimation is improved with the longer datasets. According to the Figure 1, it can be seen clealry that the variation of the data adjustment values is large in the shorter datasets. In this research, variables impacting runoff generation (c_g) appears sensitive yet again on an annual scale in the XAJ model while maintaining C_p and C_{ep} constant [34]. Therefore, this study tried to analyse the sensitiviy of recession constant estimation in accordance with the data adjustment parameter during the data scarcity. In order to prove that, the consideration of the sensitivity of recession constant over the model performance became critical.

Preprints (www.preprints.org) | NOT PEER-REVIEWED | Posted: 1 December 2023 doi:10.20944/preprints202312.0058.v1

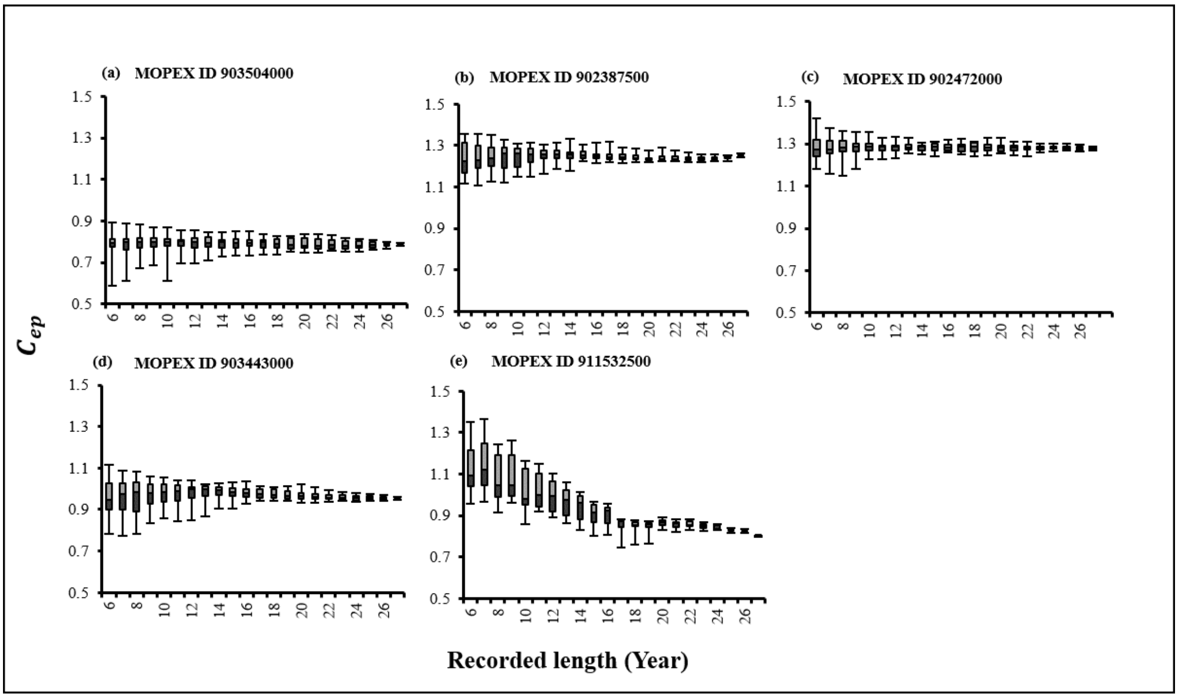

Figure 1. Box plot with C_{ep} values using 75^{th} percentile and 25^{th} percentile in MOPEX ID (a) 903504000 (b)902387500 (c) 902472000 (d) 903443000 (e) 911532500.

To highlight the recession constant sensitivity, the XAJ model calibration was performed in two approach as discussed in Section 2.8. Firstly, the model is simulated using the recession constant values ($c_{g,ref}$) optimized with longer datasets. Secondly, the model performance was checked using the recession constant for subsets ($c^{n,m}_{g,best}$).

3.1. Reference c_g for 28-Year Datasets

The pre-optimized recession constant values, ϕ_0 , in five MOPEX studied basins were initially computed based on the time constant, T, as in Equation (7), to achieve in the interval of [0,1].These c_g values were applied in the XAJ model calibration alongside with the remaining pre-optimized parameters,ϕ_0 .Relying on the annual Nash results, the estimation of simulated c_g for each basin can be assessed by using the polynomila regression analysis.

To be able to attain better calibration, model users typically employ the longest accessible data series.This study considered the simulated recession constant as the reference, as it was estimated using 28-year of datasets. However, the real issue is the information included in the datasets and how effectively that information is extracted, not the length of the dataset itself [23,49]. Therefore, estimating the C_{ep} values ($C^{n,m}_{ep}$) for shorter datasets is essential to analyze the impact of the recession constant in subsets. Figure 2 reveals the best connection values, $c_{g,ref}$, comparing the annual Nash, NSE, and the pre-optimized c_g values.

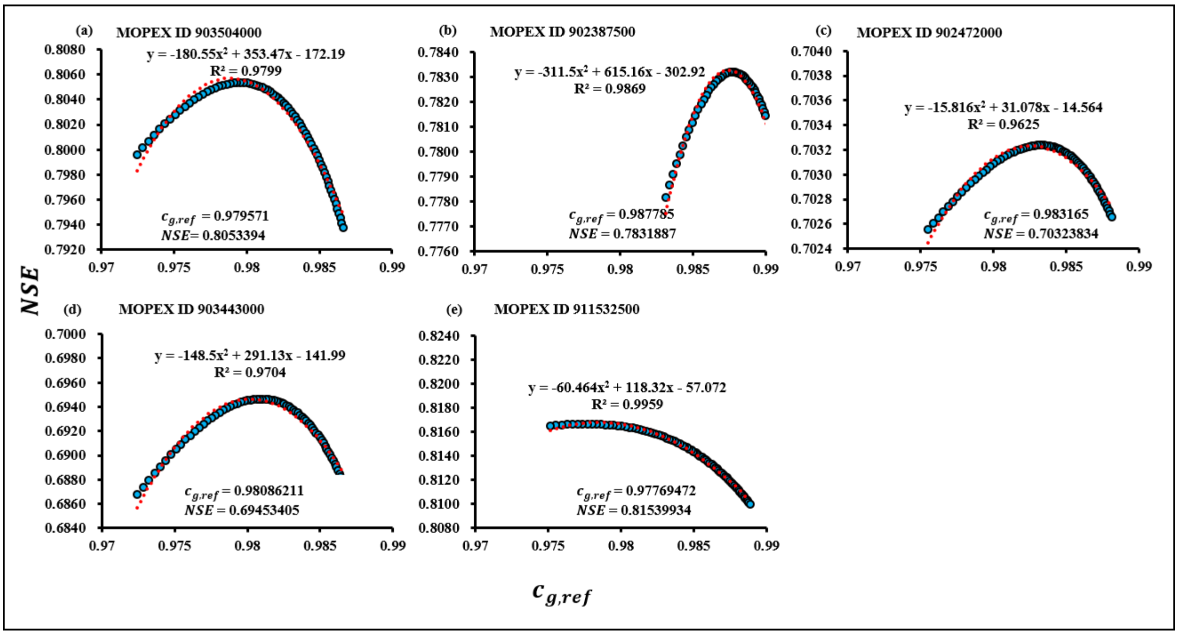

Figure 2. Estimation of reference c_g ($c_{g,ref}$) from annual Nash *NSE* results using 28-year of datasets in MOPEX ID (a) 903504000 (b)902387500 (c) 902472000 (d) 903443000 (e) 911532500.

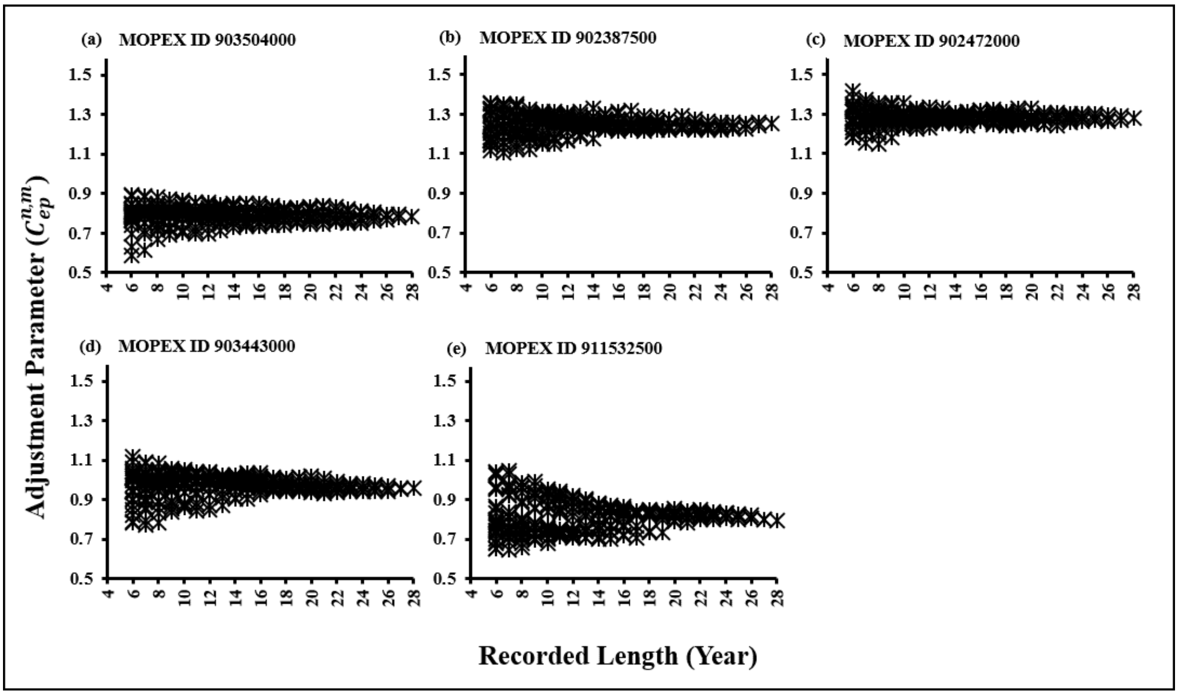

Figure 3. Estimation of C_{ep} for subsets in MOPEX ID (a) 903504000 (b)902387500 (c) 902472000 (d) 903443000 (e) 911532500.

3.2. Derivation of Data Adjustment Parameter ($C_{ep}^{n,m}$)

To compare the sensitivity of the recession constant over the data adjustment parameter for consecutive subsets ($I^{n,m}$) it was essential to evaluate the initial model performance values of *NSE* applying with $C_{ep}^{n,m}$ and $c_{g,ref}$.

Firstly, the value of $C_{ep}^{n,m}$ is classified into three categories based on the model (*NSE*) values calibrated using the reference $c_{g,ref}$ in each subset, $I^{n,m}$:

Preprints (www.preprints.org) | NOT PEER-REVIEWED | Posted: 1 December 2023 doi:10.20944/preprints202312.0058.v1

(i) $C^{n,m}_{ep,best}$ (selected when the annual Nash values,NSE, are highest after the model calibration with $c_{g,ref}$ in each subset, $I^{n,m}$);
(ii) $C^{n,m}_{ep,median}$ (selected when the annual Nash values,NSE, are median after the model calibration with $c_{g,ref}$ in each subset, $I^{n,m}$) and
(iii) $C^{n,m}_{ep,worst}$ (selected when the annual Nash values,NSE, are lowest after the model calibration with $c_{g,ref}$ in each subset, $I^{n,m}$)

Subsequently, the polynomial regression analysis was conducted to determine the corresponding $c^{n,m}_{g}$ for subsets in each category ($c^{n,m}_{g,best}$, $c^{n,m}_{g,median}$ and $c^{n,m}_{g,worst}$)(Figure 4, 6, 8).

3.3. Comparative Evaluation of Annual Nash Results, NSE, using $c^{n,m}_{g,best}$ and $C^{n,m}_{ep,best}$ in Subsets

After the model calibration using the reference c_g, the C_{ep} ($C^{n,m}_{ep,best}$) resulted from the highest annual Nash results were selected for each subsets as shown in Table 4.

Firstly,it is observed that as the data length increases, the NSE values derived from both $c_{g,ref}$ and $c^{n,m}_{g,best}$ exhibit a declining trend. As indicated in Table, this implies that longer datasets might struggle to align with the model's best performance. In the contrary, the 6-year subsets display the most significant upward trends in NSE results, attributed to shorter datasets being more compatible with $c^{n,m}_{g,best}$. Beyond this trend pattern, a comparison was conducted between NSE values in subsets when using $c_{g,ref}$ and $c^{n,m}_{g,best}$ as shown in Figure 3.

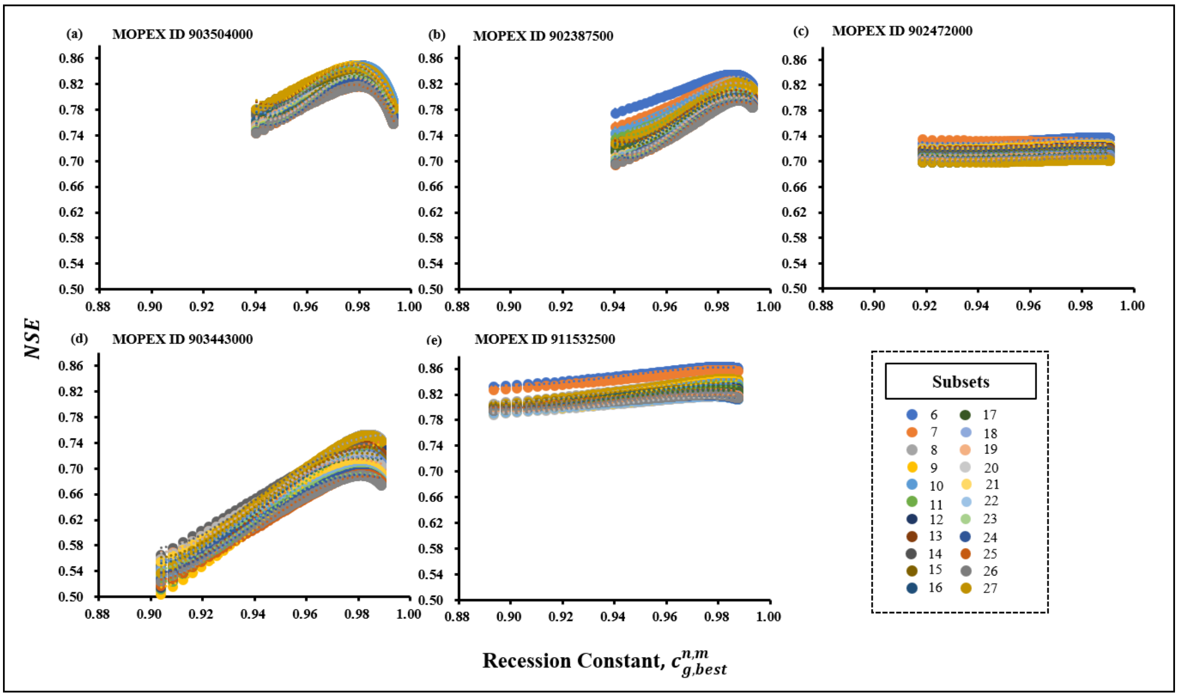

Figure 4. Estimation of $c^{n,m}_{g,best}$ for subsets by using linear polynomial regression analysis in MOPEX ID (a) 903504000 (b)902387500 (c) 902472000 (d) 903443000 (e) 911532500.

According to Figure , the NSE curves in each subset showed a relative increase while running the model with $c^{n,m}_{g,best}$. However, no significant difference between the curves of NSE resulted from the model calibration using both $c_{g,ref}$ and $c^{n,m}_{g,best}$. In other words, the results suggest little space for improving the model performance while running the model with $c^{n,m}_{g,best}$. Therefore, the impact of the sensitivity of $c^{n,m}_{g,best}$ over C_{ep} in parameter estimation can be considered limited. Consequently, the potential impact of the sensitivity of $c^{n,m}_{g,best}$ can also be limited to the performance of the model as well as the minimum data length estimation. On the other hand, the recent estimation of the minimum data

Preprints (www.preprints.org) | NOT PEER-REVIEWED | Posted: 1 December 2023 doi:10.20944/preprints202312.0058.v1

length remains consistent while considering the sensitivity of parameter estimation with c_g considering best parameter optimization scenario in subsets.

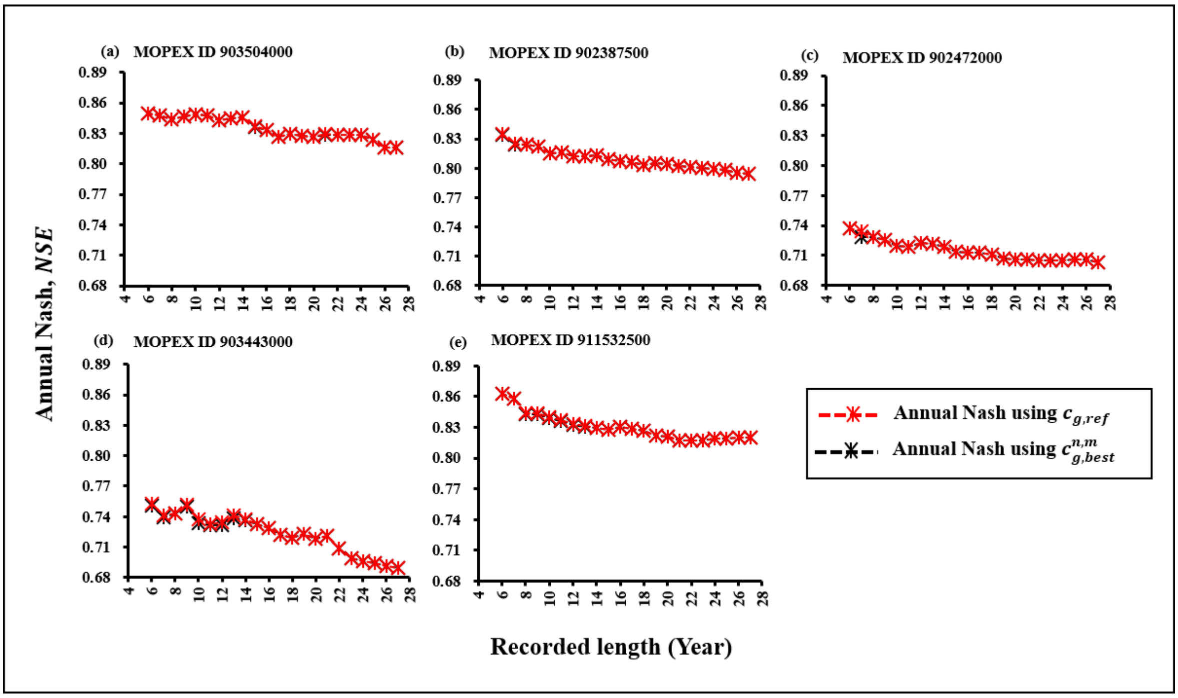

Figure 5. Comparison of Nash values using $c_{g,ref}$ and $c^{n,m}_{g,best}$ for subsets in MOPEX ID (a) 903504000 (b)902387500 (c) 902472000 (d) 903443000 (e) 911532500.

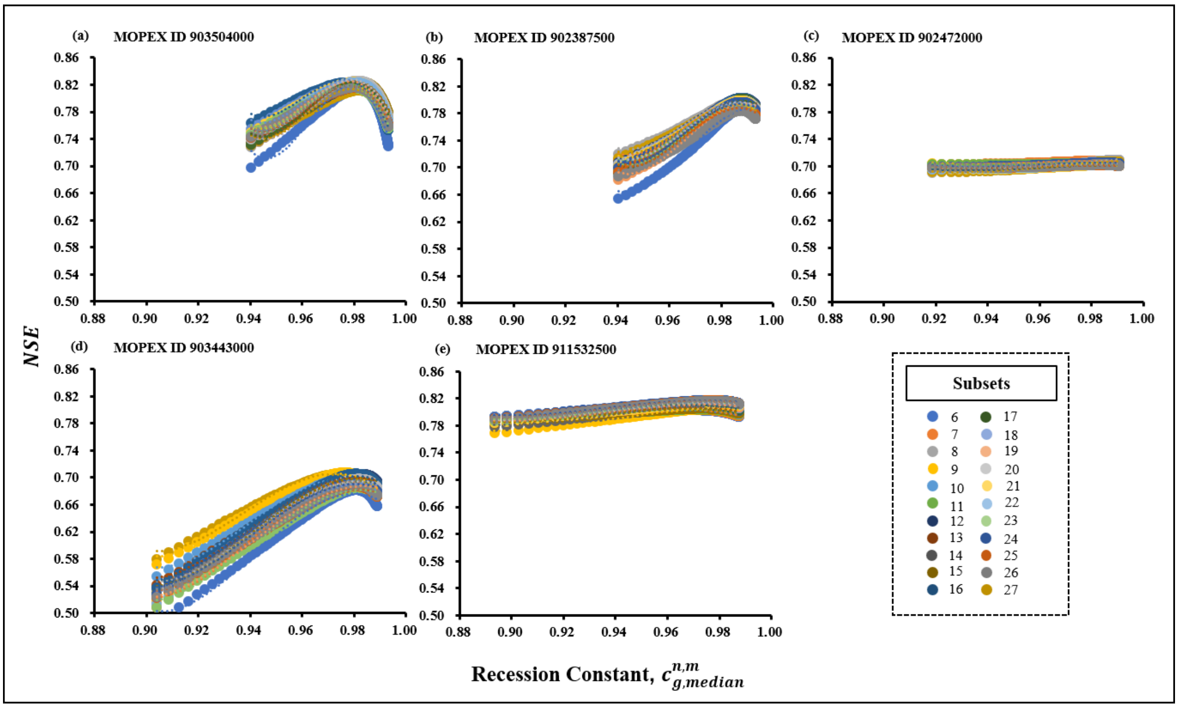

Figure 6. Estimation of $c^{n,m}_{g,median}$ for subsets by using linear polynomial regression analysis in MOPEX ID (a) 903504000 (b)902387500 (c) 902472000 (d) 903443000 (e) 911532500.

Preprints (www.preprints.org) | NOT PEER-REVIEWED | Posted: 1 December 2023 doi:10.20944/preprints202312.0058.v1

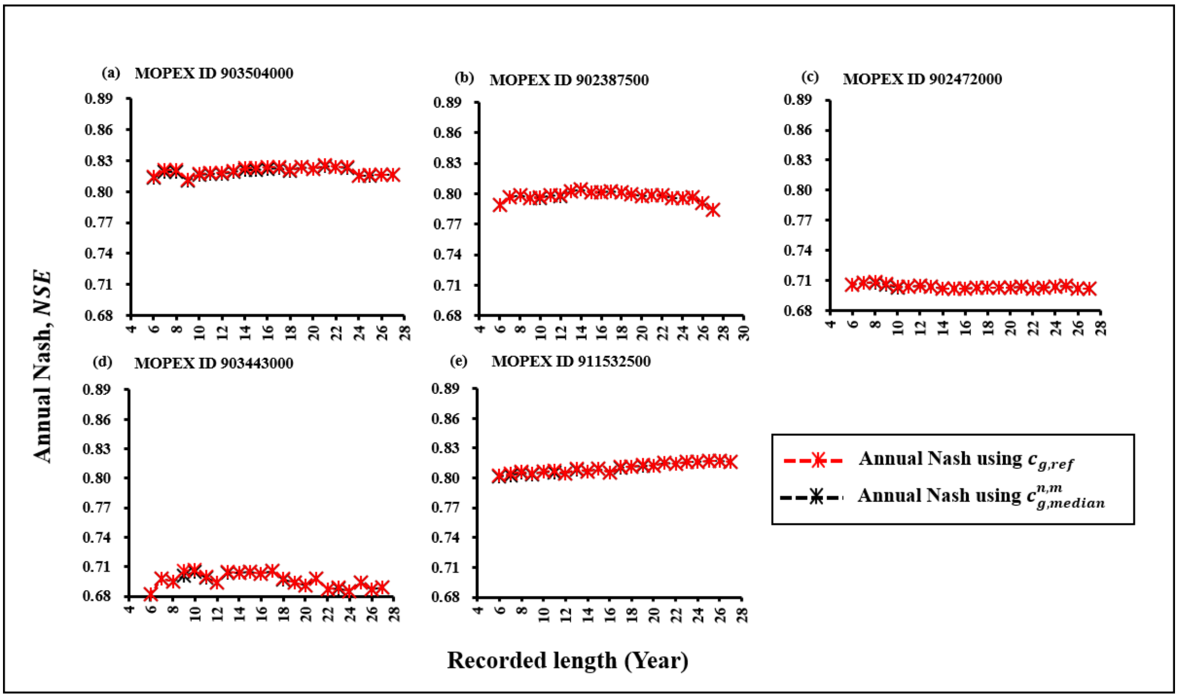

Figure 7. Comparison of Nash reulsts using $c_{g,ref}$ and $c^{n,m}_{g,median}$ for subsets in MOPEX ID (a) 903504000 (b)902387500 (c) 902472000 (d) 903443000 (e) 911532500.

Table 4. Detail Description of $c^{n,m}_{g,best}$ and $c^{n,m}_{g,best}$ values in MOPEX ID (a) 903504000 (b)902387500 (c) 902472000 (d) 903443000 (e) 911532500.

Subsets	MOPEX ID									
	9903504000		9902387500		9902472000		9903443000		9911532500	
	$C_{ep,best}$	$c^{n,m}_{g,best}$	$C_{ep,best}$	$c_{g,best}$	$C_{ep,best}$	$c_{g,best}$	$C_{ep,best}$	$c_{g,best}$	$C_{ep,best}$	$c_{g,best}$
6	0.8189	0.979725	1.3559	0.98548	1.3108	0.98496	1.1154	0.98386	0.8562	0.98106
7	0.7970	0.979725	1.3500	0.98644	1.2181	0.91861	1.0891	0.98411	0.8353	0.98122
8	0.7810	0.978669	1.3524	0.98728	1.2805	0.98333	1.0831	0.98318	0.9835	0.98197
9	0.7937	0.978669	1.2974	0.98791	1.3074	0.98300	1.037	0.98359	0.9933	0.98253
10	0.7883	0.979033	1.3009	0.98791	1.3065	0.98333	1.0529	0.98460	0.9504	0.98293
11	0.8095	0.980980	1.2574	0.98597	1.2712	0.98411	1.0226	0.98260	0.9298	0.98293
12	0.8043	0.978669	1.2611	0.98644	1.2699	0.98365	1.0405	0.98411	0.9108	0.98212
13	0.7763	0.978669	1.2684	0.98687	1.2688	0.98300	1.0123	0.98411	0.8969	0.98226
14	0.7737	0.978669	1.2394	0.98728	1.2874	0.98282	0.991	0.98245	0.8732	0.97894
15	0.7666	0.978292	1.2292	0.98687	1.2843	0.98333	0.972	0.98060	0.8548	0.97791
16	0.7783	0.979725	1.2559	0.98728	1.2673	0.98365	0.96	0.98131	0.8634	0.97875
17	0.7955	0.979385	1.2197	0.98741	1.2666	0.98317	0.9566	0.98165	0.846	0.97952
18	0.7864	0.980054	1.2253	0.98741	1.2847	0.98349	0.9615	0.98131	0.8394	0.97970
19	0.7810	0.980054	1.2428	0.98754	1.2462	0.98191	0.9463	0.98149	0.8321	0.97875
20	0.7959	0.980054	1.2398	0.98766	1.2638	0.98229	0.9451	0.97982	0.8267	0.97894
21	0.7880	0.980681	1.2324	0.98741	1.3095	0.98454	0.932	0.98022	0.8095	0.97875
22	0.7959	0.980980	1.2268	0.98754	1.3090	0.98454	0.9377	0.98041	0.8475	0.97769
23	0.8087	0.981270	1.2249	0.98766	1.2804	0.98468	0.941	0.98060	0.8403	0.97701
24	0.8115	0.981270	1.2335	0.98791	1.2863	0.98482	0.9436	0.98096	0.8083	0.97629
25	0.8059	0.980681	1.2315	0.98802	1.3000	0.98454	0.9405	0.98096	0.7995	0.97552
26	0.7897	0.980054	1.2492	0.98802	1.2984	0.98426	0.9702	0.98198	0.8064	0.97629
27	0.7931	0.980054	1.2606	0.98791	1.2888	0.98396	0.9505	0.98096	0.7972	0.97701

3.4. Comparative Evaluation of Median $c^{n,m}_g$ ($c^{n,m}_{g,median}$) Results with Annual Nash (NSE) in Subsets

In this section, the values of C_{ep} ($C^{n,m}_{ep,median}$) were selected based on the median values of model output (NSE) after the model calibration with $c_{g,ref}$ for 28-year of datasets, as shown in Table 5. After the $C^{n,m}_{ep,median}$ selection with the model outputs using $c_{g,ref}$, the calibration of the model was performed

Preprints (www.preprints.org) | NOT PEER-REVIEWED | Posted: 1 December 2023 doi:10.20944/preprints202312.0058.v1

in order to achieve the relationship between *NSE* with $c^{n,m}_{g,median}$ results. In Figure 6, the $c^{n,m}_{g,median}$ can be assumed by the model output (*NSE*) using the linear polynomial regression analysis. Here, while taking the c_g values in the median range, the trend of the *NSE* values in all subsets for all studied basins has slightly increased as the data length increased.

While considering c_g values within the median parameter optimization performance scenario, *NSE* values show a slight upward trend across all subsets as data length increases. Furthermore, *NSE* values when utilizing $c^{n,m}_{g,median}$ are slightly higher than those with $c_{g,ref}$. Despite this minor difference, it is reasonable to conclude that model outcomes using median values did not indicate any limitations over the model performance while calibrating during the data scarcity as indicated in Figure 7.

Table 5. Detail Description of $C^{n,m}_{ep,median}$ and $c^{n,m}_{g,median}$ values in MOPEX ID (a) 903504000 (b)902387500 (c) 902472000 (d) 903443000 (e) 911532500.

Subsets	MOPEX ID									
	903504000		902387500		902472000		903443000		911532500	
	$C_{ep,median}$	$c_{g,median}$	$C_{ep,median}$	$c_{g,median}$	$C_{ep,median}$	$c_{g,median}$	$C_{ep,median}$	$c_{g,median}$	$C_{ep,median}$	$c_{g,median}$
6	0.8852	0.97116	1.2602	0.98937	1.2648	0.98229	1.0093	0.98078	0.6528	0.96957
7	0.8840	0.97116	1.2397	0.98644	1.2654	0.98229	1.0336	0.98022	0.6465	0.96640
8	0.8811	0.97182	1.1995	0.98673	1.3409	0.98904	0.8624	0.97941	0.7498	0.97037
9	0.8167	0.97306	1.2783	0.98673	1.3468	0.98852	0.836	0.97509	0.7287	0.97254
10	0.8079	0.97364	1.2863	0.98728	1.2288	0.97604	0.8684	0.97654	0.9082	0.97914
11	1.0000	0.97419	1.2478	0.98779	1.2429	0.98152	0.8674	0.97782	0.7455	0.96829
12	0.8000	0.97472	1.2394	0.98728	1.2321	0.98022	0.9259	0.98096	0.7268	0.97350
13	0.8379	0.97572	1.1886	0.98802	1.2627	0.98396	1.006	0.98304	0.7081	0.97075
14	0.8302	0.97572	1.2704	0.98825	1.273	0.98426	0.9633	0.98096	0.7092	0.97254
15	0.8182	0.97619	1.2547	0.98814	1.2608	0.98426	0.9652	0.98131	0.8439	0.97791
16	0.8486	0.97619	1.3136	0.98802	1.2845	0.98559	0.962	0.98149	0.7697	0.97350
17	0.7506	0.97619	1.2419	0.98791	1.2926	0.98583	0.9467	0.98078	0.708	0.97185
18	0.8241	0.97664	1.2386	0.98802	1.2902	0.98411	0.9685	0.98165	0.7311	0.97254
19	0.7801	0.97708	1.2414	0.98741	1.258	0.98426	0.965	0.98198	0.735	0.97319
20	0.7816	0.97750	1.2764	0.98847	1.2874	0.98468	0.967	0.98230	0.8224	0.97701
21	0.8303	0.97790	1.2425	0.98791	1.2762	0.98396	0.9548	0.98182	0.8302	0.97769
22	0.7824	0.97790	1.2532	0.98741	1.2884	0.98522	0.9438	0.98131	0.8179	0.97834
23	0.7902	0.97829	1.2389	0.98802	1.2877	0.98509	0.9827	0.98182	0.8161	0.97701
24	0.7694	0.97867	1.2558	0.98754	1.3018	0.98482	0.9566	0.98182	0.8304	0.97854
25	0.7933	0.97867	1.2567	0.98754	1.2852	0.98454	0.9405	0.98096	0.8137	0.97724
26	0.7965	0.97903	1.2511	0.98754	1.2637	0.98317	0.9441	0.98078	0.8039	0.97791
27	0.7931	0.97938	1.2413	0.98766	1.2699	0.98349	0.9505	0.98096	0.801	0.97791

Preprints (www.preprints.org) | NOT PEER-REVIEWED | Posted: 1 December 2023 doi:10.20944/preprints202312.0058.v1

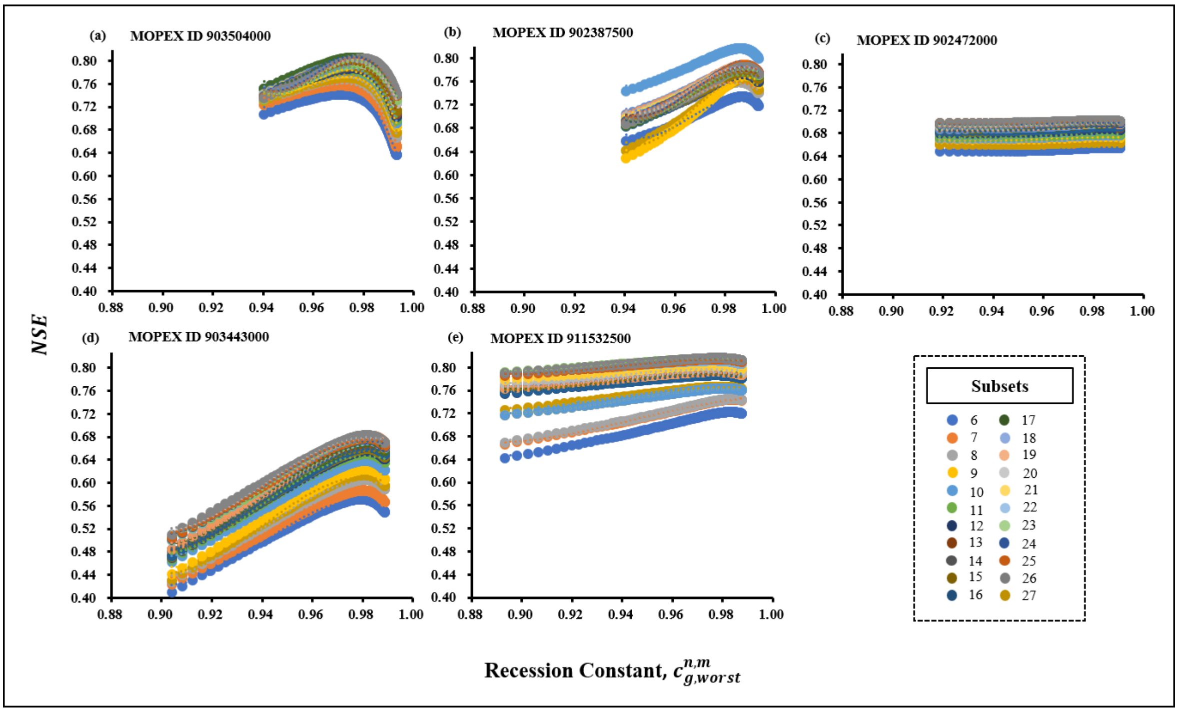

Figure 8. Estimation of $c_{g,worst}^{n,m}$ for subsets by using linear polynomial regression analysis in MOPEX ID (a) 903504000 (b)902387500 (c) 902472000 (d) 903443000 (e) 911532500.

3.5. Comparative Assessment of Annual Nash results, NSE, Using $c_{g,worst}^{n,m}$ and $C_{ep,best}^{n,m}$ in Subsets

According to [50], to estimate the most sensitive parameter, it can be considered both the best and worse condition for the sensitivity analysis for the parameter optimization. However, to expect good model performance, the worst condition for the parameter optimization is essential to take into consideration.This approach achieving strong model performance under challenging conditions is imperative.A significant difference is evident when comparing *NSE* values obtained from the two categories (best and median) with those from $c_{g,worst}^{n,m}$ and $c_{g,ref}$. This result showed the significant impact over the model performance by utilizing *NSE* values with $c_{g,worst}^{n,m}$. Unlike the previously mentioned categories, the influence of c_g on the estimation of C_{ep} becomes pronounced in the worst-case scenario (Figure 4). Additionally, the sensitivity of c_g further magnifies its impact on model performance under these conditions. The insight provided by Figure 9 clearly illustrates the variations in *NSE* values among the three categories across all studied basins.

 doi:10.20944/preprints202312.0058.v1

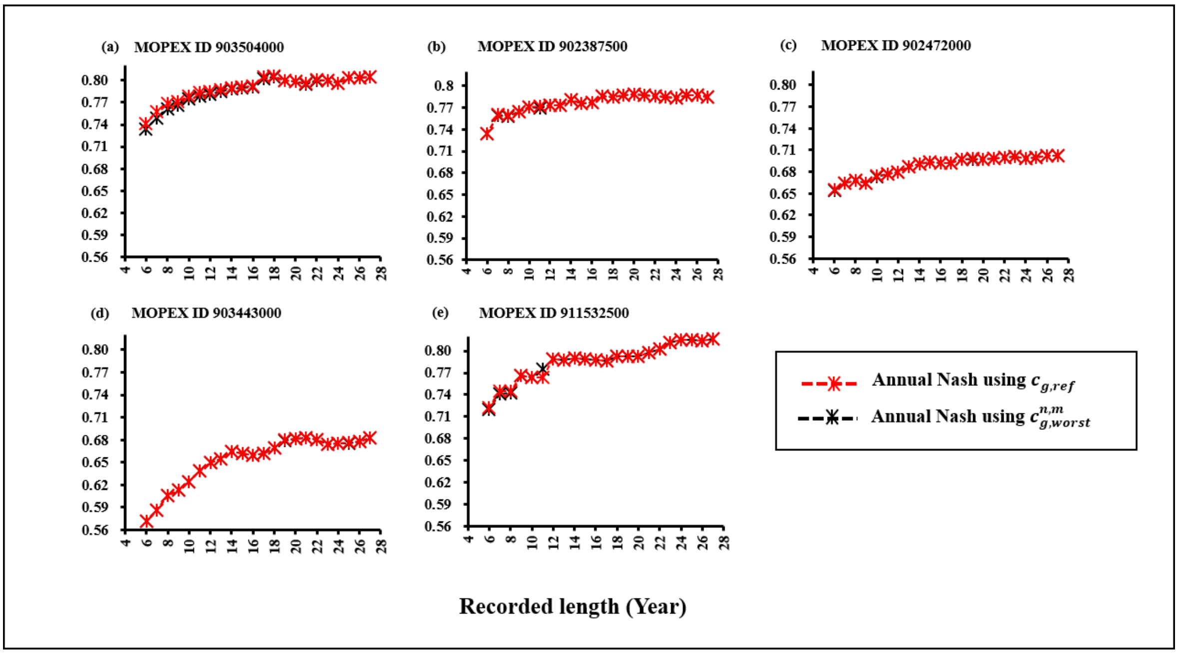

Figure 9. Comparison of Nash using $c_{g,ref}$ and $c^{n,m}_{g,worst}$ for subsets in MOPEX ID (a) 903504000 (b)902387500 (c) 902472000 (d) 903443000 (e) 911532500.

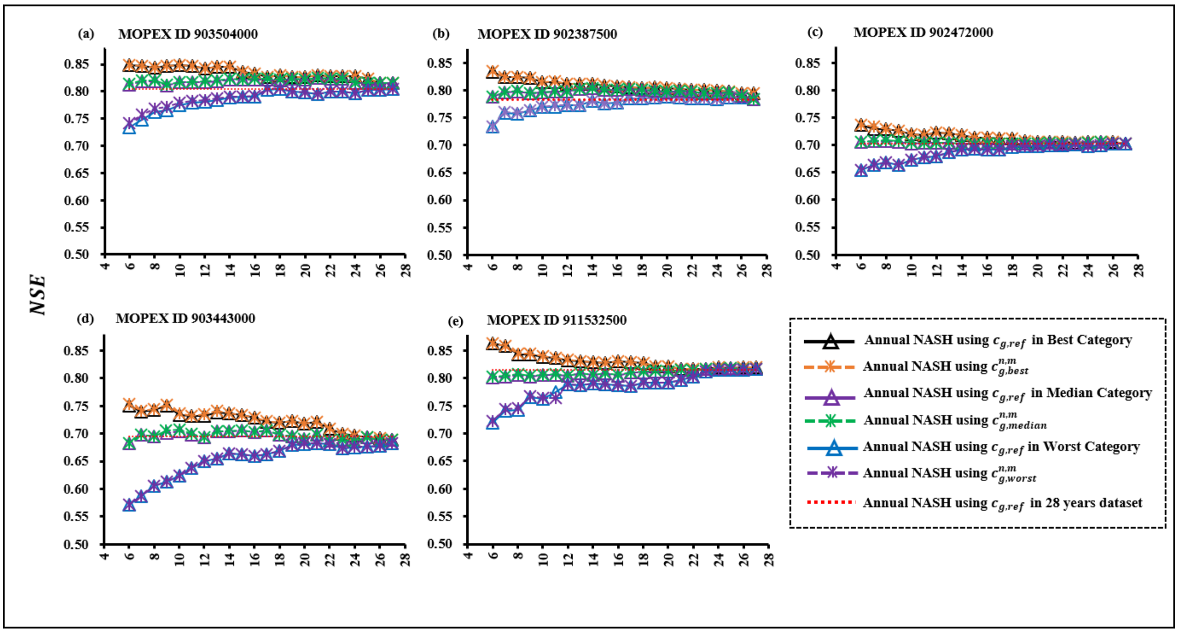

Figure 10. Comparison of annual Nash in subsets based on all three categories ($c^{n,m}_{g,best}$, $c^{n,m}_{g,median}$ and $c^{n,m}_{g,worst}$) in MOPEX ID (a) 903504000 (b)902387500 (c) 902472000 (d) 903443000 (e) 911532500.

Table 6. Detail Description of $C^{n,m}_{ep,worst}$ and $c^{n,m}_{g,worst}$ values in MOPEX ID (a) 903504000 (b)902387500 (c) 902472000 (d) 903443000 (e) 911532500.

Subsets	MOPEX ID 903504000		902387500		902472000		903443000		911532500	
	$C_{ep,worst}$	$c_{g,worst}$	$C_{ep,worst}$	$c_{g,worst}$	$C_{ep,worst}$	$c_{g,worst}$	$C_{ep,worst}$	$c_{g,worst}$	$C_{ep,worst}$	$c_{g,worst}$
6	0.5869	0.98155	1.1664	0.98673	1.3523	0.98702	0.9408	0.97941	0.9584	0.98318
7	0.6114	0.98235	1.1331	0.98548	1.2522	0.98411	0.9662	0.98022	0.9644	0.98413
8	0.6705	0.98235	1.1894	0.98548	1.2689	0.98381	0.9467	0.98096	0.9351	0.98413
9	0.6877	0.98182	1.2826	0.98728	1.2907	0.98426	0.952	0.98060	0.8556	0.97952
10	0.6992	0.98098	1.2653	0.98825	1.3156	0.98522	0.9688	0.98096	0.8752	0.98058
11	0.6954	0.98182	1.2574	0.98597	1.2822	0.98547	0.9863	0.98114	0.8559	0.98058
12	0.6940	0.98155	1.1682	0.98687	1.311	0.98496	0.9907	0.98131	0.8166	0.97678
13	0.7099	0.98209	1.1957	0.98715	1.3273	0.98559	0.9997	0.98165	0.8366	0.97791
14	0.7289	0.98235	1.1779	0.98741	1.3046	0.98534	1.0104	0.98165	0.7986	0.97653
15	0.7337	0.98209	1.2303	0.98754	1.3123	0.98702	0.9983	0.98214	0.815	0.97701
16	0.7322	0.98260	1.2374	0.98754	1.3199	0.98692	0.9905	0.98182	0.8059	0.97653
17	0.7379	0.97750	1.2769	0.98754	1.3247	0.98672	0.9973	0.98198	0.8224	0.97747
18	0.7377	0.98182	1.2919	0.98741	1.3103	0.98692	1.0057	0.98198	0.8428	0.97724
19	0.7517	0.97972	1.2381	0.98715	1.3158	0.98712	1.014	0.98317	0.8347	0.97653
20	0.7450	0.98037	1.2190	0.98741	1.2928	0.98454	0.9987	0.98275	0.8278	0.97701
21	0.7474	0.98155	1.2240	0.98754	1.2918	0.98454	0.9687	0.98165	0.805	0.97678
22	0.7543	0.98005	1.2330	0.98754	1.265	0.98349	0.9558	0.98198	0.7971	0.97578
23	0.7510	0.98037	1.2326	0.98766	1.2587	0.98265	0.9592	0.98182	0.8002	0.97604
24	0.7526	0.97938	1.2303	0.98766	1.2779	0.98349	0.9655	0.98198	0.8067	0.97653
25	0.7591	0.98037	1.2255	0.98754	1.2717	0.98282	0.9467	0.98131	0.8231	0.97791
26	0.7672	0.98037	1.2239	0.98766	1.2755	0.98426	0.9531	0.98149	0.8193	0.97813
27	0.7797	0.98005	1.2413	0.98766	1.2699	0.98349	0.9608	0.98149	0.801	0.97791

4. Conclusion

This study presents an overview of the crucial role of recession constant sensitivity with the data adjustment parameter in parameter estimation using the XAJ model. Linear polynomial regression analysis is tested, utilizing 28-year U.S. MOPEX datasets and subsets from five river basins. The objective of this paper was to identify the recession constant sensitivity in parameter estimation can result the poor model performance during the data scarcity. The data analysis results revealed that the potential impact of recession constant and its interaction with data adjustment parameter are limited in longer datasets. While recession constant sensitivity moderately impacts model performance in shorter datasets, a significant difference in model performance is observed while calibrating the model in the worst scenario. This analysis indicates that the recession constant parameter and the data adjustment parameter relationship remains robust across different data lengths even though the data adjustment parameters showed the large parameter variations in shorter datasets. Overall, in basins with limited data, it is crucial to consider the interaction of the recession constant as it can impact the model performance during the worst case scenario.

Understanding recession constant sensitivity enhances parameter estimation, improving more accurate and reliable conceptual hydrological model predictions and facilitating precise, acceptable minimum data length estimation in data scarce basins. This study can be mainly used in areas where data availability is limited to consider the recession constant sensitivity in the longer time scales. In summary, this study bridges a gap in understanding the complex interrelationships of hydrological model parameters, facilitating more precise water resource management and planning decisions.

Author Contributions: Conceptualization, T.T.Z. and M.L.; methodology, T.T.Z. and M.L.; software, T.T.Z.; validation, T.T.Z.; formal analysis, T.T.Z.; investigation, T.T.Z. and M.L.; resources, M.L.; data curation, T.T.Z. and M.L.; writing—original draft preparation, T.T.Z.; writing—review and editing, T.T.Z. and M.L.; visualization, T.T.Z.; supervision, M.L.; project administration, M.L. All authors have read and agreed to the published version of the manuscript.

Funding: This research received no external funding.

Institutional Review Board Statement: Not applicable.

 doi:10.20944/preprints202312.0058.v1

Informed Consent Statement: Not applicable.

Data Availability Statement: Information on all the data applied in this research is shown in Section 2

Conflicts of Interest: Regarding this paper and the research, the authors state that they have no conflicts of interest.

References

1. Devia, G.K.; Ganasri, B.P.; Dwarakish, G.S. A review on hydrological models. *Aquatic procedia* **2015**, *4*, 1001–1007.
2. Peel, M.C.; Blöschl, G. Hydrological modelling in a changing world. *Progress in Physical Geography* **2011**, *35*, 249–261.
3. Birkholz, S.; Muro, M.; Jeffrey, P.; Smith, H.M. Rethinking the relationship between flood risk perception and flood management. *Science of the total environment* **2014**, *478*, 12–20.
4. Adikari, Y.; Yoshitani, J. Global trends in water-related disasters: an insight for policymakers. *World Water Assessment Programme Side Publication Series, Insights. The United Nations, UNESCO. International Centre for Water Hazard and Risk Management (ICHARM)* **2009**, pp. 1–24.
5. Modarres, R.; Ouarda, T.B. Modeling rainfall–runoff relationship using multivariate GARCH model. *Journal of Hydrology* **2013**, *499*, 1–18.
6. Loucks, D.P.; Van Beek, E. *Water resource systems planning and management: An introduction to methods, models, and applications*; Springer, 2017.
7. Refsgaard, J.C.; Knudsen, J. Operational validation and intercomparison of different types of hydrological models. *Water resources research* **1996**, *32*, 2189–2202.
8. Ramos, M.H.; Mathevet, T.; Thielen, J.; Pappenberger, F. Communicating uncertainty in hydro-meteorological forecasts: mission impossible? *Meteorological Applications* **2010**, *17*, 223–235.
9. Raje, D.; Krishnan, R. Bayesian parameter uncertainty modeling in a macroscale hydrologic model and its impact on Indian river basin hydrology under climate change. *Water Resources Research* **2012**, *48*.
10. Zhao, F.; Wu, Y.; Qiu, L.; Sun, Y.; Sun, L.; Li, Q.; Niu, J.; Wang, G. Parameter uncertainty analysis of the SWAT model in a mountain-loess transitional watershed on the Chinese Loess Plateau. *Water* **2018**, *10*, 690.
11. Wu, Y.; Liu, S.; Huang, Z.; Yan, W. Parameter optimization, sensitivity, and uncertainty analysis of an ecosystem model at a forest flux tower site in the United States. *Journal of Advances in Modeling Earth Systems* **2014**, *6*, 405–419.
12. Bárdossy, A.; Singh, S. Robust estimation of hydrological model parameters. *Hydrology and earth system sciences* **2008**, *12*, 1273–1283.
13. Renard, B.; Kavetski, D.; Kuczera, G.; Thyer, M.; Franks, S.W. Understanding predictive uncertainty in hydrologic modeling: The challenge of identifying input and structural errors. *Water Resources Research* **2010**, *46*.
14. Muleta, M.K.; Nicklow, J.W. Sensitivity and uncertainty analysis coupled with automatic calibration for a distributed watershed model. *Journal of hydrology* **2005**, *306*, 127–145.
15. Jeremiah, E.; Sisson, S.A.; Sharma, A.; Marshall, L. Efficient hydrological model parameter optimization with Sequential Monte Carlo sampling. *Environmental Modelling & Software* **2012**, *38*, 283–295.
16. Celeux, G.; Hurn, M.; Robert, C.P. Computational and inferential difficulties with mixture posterior distributions. *Journal of the American Statistical Association* **2000**, *95*, 957–970.
17. Arnold, J.G.; Youssef, M.A.; Yen, H.; White, M.J.; Sheshukov, A.Y.; Sadeghi, A.M.; Moriasi, D.N.; Steiner, J.L.; Amatya, D.M.; Skaggs, R.W.; et al. Hydrological processes and model representation: impact of soft data on calibration. *Transactions of the ASABE* **2015**, *58*, 1637–1660.
18. Bates, B.C.; Campbell, E.P. A Markov chain Monte Carlo scheme for parameter estimation and inference in conceptual rainfall-runoff modeling. *Water resources research* **2001**, *37*, 937–947.
19. Vrugt, J.A.; Ter Braak, C.J.; Clark, M.P.; Hyman, J.M.; Robinson, B.A. Treatment of input uncertainty in hydrologic modeling: Doing hydrology backward with Markov chain Monte Carlo simulation. *Water Resources Research* **2008**, *44*.
20. Gottschalk, F.; Sun, T.; Nowack, B. Environmental concentrations of engineered nanomaterials: review of modeling and analytical studies. *Environmental pollution* **2013**, *181*, 287–300.

Preprints (www.preprints.org) | NOT PEER-REVIEWED | Posted: 1 December 2023 doi:10.20944/preprints202312.0058.v1

21. Kuczera, G.; Parent, E. Monte Carlo assessment of parameter uncertainty in conceptual catchment models: the Metropolis algorithm. *Journal of hydrology* **1998**, *211*, 69–85.
22. Micevski, T.; Kuczera, G. Combining site and regional flood information using a Bayesian Monte Carlo approach. *Water Resources Research* **2009**, *45*.
23. Sorooshian, S.; Gupta, V.K. Automatic calibration of conceptual rainfall-runoff models: The question of parameter observability and uniqueness. *Water resources research* **1983**, *19*, 260–268.
24. Thyer, M.; Renard, B.; Kavetski, D.; Kuczera, G.; Franks, S.W.; Srikanthan, S. Critical evaluation of parameter consistency and predictive uncertainty in hydrological modeling: A case study using Bayesian total error analysis. *Water Resources Research* **2009**, *45*.
25. Wagener, T.; McIntyre, N.; Lees, M.; Wheater, H.; Gupta, H. Towards reduced uncertainty in conceptual rainfall-runoff modelling: Dynamic identifiability analysis. *Hydrological processes* **2003**, *17*, 455–476.
26. Bergström, S. Principles and confidence in hydrological modelling. *Hydrology Research* **1991**, *22*, 123–136.
27. Beven, K.J. *Rainfall-runoff modelling: the primer*; John Wiley & Sons, 2011.
28. Lu, M. Recent and future studies of the Xinanjiang Model. *J. Hydraul. Eng* **2021**, *52*, 432–441.
29. Singh, V.P.; et al. *Computer models of watershed hydrology*; Vol. 1130, Water resources publications Highlands Ranch, CO, 1995.
30. Gan, Y.; Duan, Q.; Gong, W.; Tong, C.; Sun, Y.; Chu, W.; Ye, A.; Miao, C.; Di, Z. A comprehensive evaluation of various sensitivity analysis methods: A case study with a hydrological model. *Environmental modelling & software* **2014**, *51*, 269–285.
31. Zin, T.T.; Lu, M. Influence of Data Length on the Determination of Data Adjustment Parameters in Conceptual Hydrological Modeling: A Case Study Using the Xinanjiang Model. *Water* **2022**, *14*, 3012.
32. Schaake, J.; Cong, S.; Duan, Q. US MOPEX data set. Technical report, Lawrence Livermore National Lab.(LLNL), Livermore, CA (United States), 2006.
33. Ren-Jun, Z. The Xinanjiang model applied in China. *Journal of hydrology* **1992**, *135*, 371–381.
34. Lu, M.; Li, X. Time scale dependent sensitivities of the XinAnJiang model parameters. *Hydrological Research Letters* **2014**, *8*, 51–56.
35. Hapuarachchi, H.; Li, Z.; Wang, S. Application of SCE-UA method for calibrating the Xinanjiang watershed model. *Journal of Lake Sciences* **2001**, *13*, 304–314.
36. Zhao, R.; Liu, X. The Xinanjiang Model, Computer Models of Watershed Hydrology; Singh, VP, Ed, 1995.
37. Li, X.; Lu, M. Application of aridity index in estimation of data adjustment parameters in the Xinanjiang model. 土木論文集 *B1 (水工)* **2014**, *70*, I_163–I_168.
38. Garrick, M.; Cunnane, C.; Nash, J. A criterion of efficiency for rainfall-runoff models. *Journal of Hydrology* **1978**, *36*, 375–381.
39. Gupta, H.V.; Kling, H.; Yilmaz, K.K.; Martinez, G.F. Decomposition of the mean squared error and NSE performance criteria: Implications for improving hydrological modelling. *Journal of hydrology* **2009**, *377*, 80–91.
40. Gupta, H.V.; Kling, H. On typical range, sensitivity, and normalization of Mean Squared Error and Nash-Sutcliffe Efficiency type metrics. *Water Resources Research* **2011**, *47*.
41. Houghton-Carr, H. Assessment criteria for simple conceptual daily rainfall-runoff models. *Hydrological Sciences Journal* **1999**, *44*, 237–261.
42. McCuen, R.H.; Knight, Z.; Cutter, A.G. Evaluation of the Nash–Sutcliffe efficiency index. *Journal of hydrologic engineering* **2006**, *11*, 597–602.
43. Schaefli, B.; Gupta, H.V. Do Nash values have value? *Hydrological processes* **2007**, *21*, 2075–2080.
44. Nash, J.E.; Sutcliffe, J.V. River flow forecasting through conceptual models part I—A discussion of principles. *Journal of hydrology* **1970**, *10*, 282–290.
45. Kutner, M.H. Applied linear statistical models. *(No Title)* **2005**.
46. Burden, R.L.; Faires, J.D.; Burden, A.M. *Numerical analysis*; Cengage learning, 2015.
47. Ostertagová, E. Modelling using polynomial regression. *Procedia Engineering* **2012**, *48*, 500–506.
48. McCuen, R.H. The role of sensitivity analysis in hydrologic modeling. *Journal of hydrology* **1973**, *18*, 37–53.
49. Li, C.z.; Wang, H.; Liu, J.; Yan, D.h.; Yu, F.l.; Zhang, L. Effect of calibration data series length on performance and optimal parameters of hydrological model. *Water Science and Engineering* **2010**, *3*, 378–393.

 doi:10.20944/preprints202312.0058.v1

50. Li, X.; Lu, M. Multi-step optimization of parameters in the Xinanjiang model taking into account their time scale dependency. *Journal of Japan Society of Civil Engineers, Ser. B1 (Hydraulic Engineering)* **2012**, *68*, I_145–I_150.